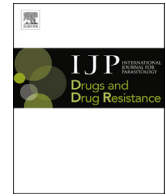




Contents lists available at ScienceDirect

International Journal for Parasitology: Drugs and Drug Resistance

journal homepage: www.elsevier.com/locate/ijpddr

Antileishmanial activity and tubulin polymerization inhibition of podophyllotoxin derivatives on *Leishmania infantum*



José Miguel Escudero-Martínez ^a, Yolanda Pérez-Pertejo ^a, Rosa M. Reguera ^a,
María Angeles Castro ^{b,*}, María Victoria Rojo ^b, Carolina Santiago ^c, Andrés Abad ^c,
Pablo Anselmo García ^b, José Luis López-Pérez ^b, Arturo San Feliciano ^b,
Rafael Balaña-Fouce ^{a,*}

^a Departamento de Ciencias Biomédicas, University of León, Campus de Vegazana s/n, 24071 León, Spain

^b Departamento de Ciencias Farmacéuticas, Área de Química Farmacéutica, Facultad de Farmacia, CIETUS, IBSAL, University of Salamanca, Campus Miguel de Unamuno s/n, 37007 Salamanca, Spain

^c Departamento de Química, Facultad de Ciencias, Universidad de Los Andes, Mérida, Venezuela

ARTICLE INFO

Article history:

Received 17 April 2017

Received in revised form

16 June 2017

Accepted 27 June 2017

Available online 28 June 2017

Dedicated to Prof. Dr. Alejandro F. Barrero

Keywords:

Leishmania

Tubulin

DNA-Topoisomerase

Podophyllotoxin

Podophyllic aldehyde

ABSTRACT

Leishmania microtubules play an important role not only in cell division, but also in keeping the shape of the parasite and motility of its free-living stages. Microtubules result from the self-assembly of alpha and beta tubulins, two phylogenetically conserved and very abundant eukaryotic proteins in kinetoplastids. The colchicine binding domain has inspired the discovery and development of several drugs currently in clinical use against parasites. However, this domain is less conserved in kinetoplastids and may be selectively targeted by new compounds. This report shows the antileishmanial effect of several series of compounds (53), derived from podophyllotoxin (a natural cyclolignan isolated from rhizomes of *Podophyllum* spp.) and podophyllic aldehyde, on a transgenic, fluorescence-emitting strain of *Leishmania infantum*. These compounds were tested on both promastigotes and amastigote-infected mouse splenocytes, and in mammalian – mouse non-infected splenocytes and liver HepG2 cells – in order to determine selective indexes of the drugs. Results obtained with podophyllotoxin derivatives showed that the hydroxyl group at position C-7 α was a structural requisite to kill the parasites. On regards podophyllic aldehyde, derivatives with C9-aldehyde group integrated into a bicyclic heterostructure displayed more potent antileishmanial effects and were relatively safe for host cells. Docking studies of podophyllotoxin and podophyllic aldehyde derivatives showed that these compounds share a similar pattern of interaction at the colchicine site of Leishmania tubulin, thus pointing to a common mechanism of action. However, the results obtained suggested that despite tubulin is a remarkable target against leishmaniasis, there is a poor correlation between inhibition of tubulin polymerization and antileishmanial effect of many of the compounds tested, fact that points to alternative pathways to kill the parasites.

© 2017 The Authors. Published by Elsevier Ltd on behalf of Australian Society for Parasitology. This is an open access article under the CC BY-NC-ND license (<http://creativecommons.org/licenses/by-nc-nd/4.0/>).

1. Introduction

Visceral leishmaniasis (VL) is a vector-borne zoonotic disease responsible for one of the most neglected diseases linked to the

Abbreviations: NTD, Neglected Tropical Diseases; VL, Visceral Leishmaniasis; AMB, Amphotericin B; AMBdc, AMB deoxicholate; iRFP, Infra Red Fluorescent Protein; FCS, Foetal Calf Serum; SI, Selectivity Index.

* Corresponding author.

** Corresponding author.

E-mail addresses: macg@usal.es (M.Á. Castro), rbalf@unileon.es (R. Balaña-Fouce).

poorest communities of low-income countries. The treatment of this disease is based on chemotherapy, since potential vaccines are in preclinical or early clinical stages of development (Beaumier et al., 2013). Current pharmacopeia against this disease includes the first line antimony derivatives (Sb^V), different formulations of the polyene fungicide amphotericin B (AMB) and the oral alkylphosphocholine miltefosine (Balaña-Fouce et al., 1998; Monge-Maillo and Lopez-Velez, 2013). These compounds have many undesirable side effects that include Sb^V cardiotoxicity (Sundar and Chakravarty, 2010), AMB nephrotoxicity (Croft and Olliaro, 2011) and the developmental toxicity of miltefosine

<http://dx.doi.org/10.1016/j.ijpddr.2017.06.003>

2211-3207/© 2017 The Authors. Published by Elsevier Ltd on behalf of Australian Society for Parasitology. This is an open access article under the CC BY-NC-ND license (<http://creativecommons.org/licenses/by-nc-nd/4.0/>).

(Bhattacharya et al., 2007). Therefore, the discovery and development of new drugs based on validated targets against VL is an urgent need, especially when Big Pharma companies have waived funds and efforts in research and development against this neglected disease.

Microtubule-targeting (antimitotic) drugs include compounds of diverse structure that can disrupt microtubule function by interacting with tubulin (Dumontet and Sikic, 1999). Microtubules are eukaryotic protein structures resulting from the polymerization of α/β -tubulin heterodimers. Microtubules are responsible for the formation of the mitotic spindle, cell shape, ciliary and flagellar motility and intracellular transport (Hawkins et al., 2010). β -Tubulin is a GTP-hydrolyzing and highly conserved protein that interacts with α -tubulin, both conforming the basic structural subunit of microtubules. Microtubules of trypanosomatids have some unique features. They are constituted by the most abundant protein in these cells, since they are responsible for the sub-pellicular corset that conforms their specific shape (Seeback et al., 1990; Kohl and Gull, 1998). In addition, they are relatively stable at low temperatures, in contrast to microtubules of many higher organisms, and they are also resistant to many drugs currently used in anthelmintic and anticancer therapies (Werbovetz, 2002). One of these drugs is colchicine, a potent inhibitor of tubulin polymerization in higher eukaryotes (Vindya et al., 2015). In mammals, colchicine binds to a β -tubulin domain located near the α/β -tubulin interface, where it prevents tubulin to adopt a straight linear structure required for further adequate polymerization (Ravelli et al., 2004). Despite β -tubulin is highly conserved from trypanosomes to other higher eukaryotic organisms, up to eleven amino acid substitutions are found in the colchicine-binding site that may explain the resistance of these parasites to such drug (Luis et al., 2013). These differences have been pointed as putative targets to be exploited in the design of new more selective polymerization inhibitors (Kaur et al., 2014).

Several drugs have been used to target trypanosomatids microtubules with low activity against mammalian counterparts. These drugs can act either by inhibiting or promoting tubulin polymerization. Dinitroaniline herbicides have shown activity against both *Leishmania* and *Trypanosoma* (Chan and Fong, 1990; Chan et al., 1991, 1993a, 1993b; Traub-Cseko et al., 2001), and tubulin has been implicated as being the target of these compounds (Chan and Fong, 1990; Chan et al., 1993b; Traub-Cseko et al., 2001). One interesting natural compound in cancer chemotherapy is podophyllotoxin (Fig. 1), an antineoplastic and antiviral cytotoxic cyclolignan isolated from *Podophyllum* spp. (Berberidaceae) and several species of other genera and families. From a mechanistic point of view, it has been demonstrated that podophyllotoxin and most of its related 4'-methoxy congeners act by inhibiting tubulin polymerization through interaction at the

colchicine-binding site (Ravelli et al., 2004), while another not yet completely defined apoptosis mechanism has been proposed for some of those compounds included in other study (Castro et al., 2010).

This article describes for the first time the evaluation of the killing effect of several series of semisynthetic podophyllotoxin derivatives on *Leishmania infantum*, the aetiological agent responsible for VL in humans and dogs in the Old World. For this purpose, an intracellular screening on macrophages isolated from naturally infected BALB/c mice with an infrared-emitting *L. infantum* strain was used. This method has the remarkable advantage of using host-infected cells under natural conditions, where splenocytes are still playing a role in the immunological response (Reguera et al., 2014). Furthermore, we have studied the potential role played by leishmanial tubulin as putative target of these compounds.

2. Material and methods

2.1. Chemistry

The chemical structures of the starting compounds podophyllotoxin and podophyllic aldehyde (Fig. 1) and the derivatives evaluated in this work are compiled in Tables (1–4). Compounds were prepared according to previous reports (Castro et al., 2004, 2010, 2012; Abad et al., 2012) and to unpublished procedures (chemical data not shown here). Their structures were respectively confirmed or assigned by either direct comparison with authentic samples, or through complete analysis of One- and Two-Dimensional ^1H and ^{13}C nuclear magnetic resonance (1D- and 2D-NMR, respectively), infrared (IR) and mass (MS) spectra for the new compounds.

2.2. Ethic statement

The animal research described in this manuscript complies with Spanish Act (RD 53/2013) and European Union Legislation (2010/63/UE). The protocols used here were approved by the Animal Care Committee of the University of León (Spain), project license number (PI12/00104).

2.3. Promastigote cultures and in vitro assays

Leishmania infantum BCN150 iRFP (henceforth referred as *L. infantum*-iRFP) is a genetically modified strain that constitutively incorporates the infrared iRFP encoding gen for infrared detection (Calvo-Álvarez et al., 2012). Promastigotes were cultured in M199 medium supplemented with 25 mM 4-(2-hydroxyethyl)-1-piperazineethanesulfonic acid (HEPES) pH 6.9, 10 mM glutamine,

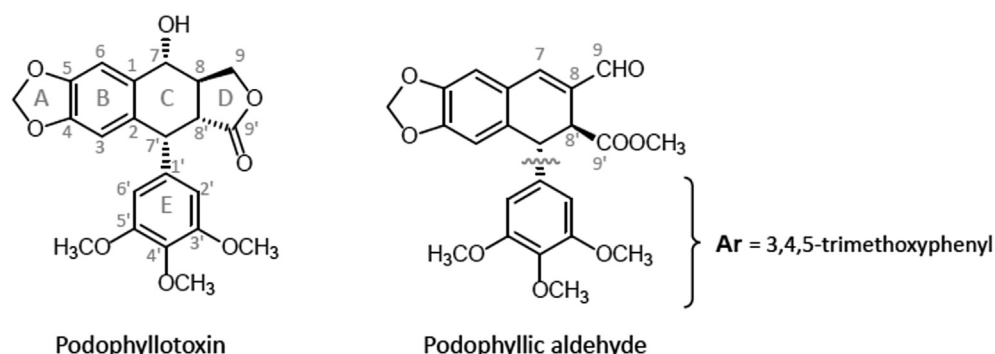


Fig. 1. Structures and numbering of positions and rings of podophyllotoxin (2a, left) and podophyllic aldehyde (14, right).

7.6 mM hemin, 0.1 mM adenosine, 0.01 mM folic acid, 1 × RPMI 1640 vitamin mix (Sigma), 10% (v/v) heat-inactivated foetal calf serum (FCS; Fisher Scientific), and antibiotic cocktail (50 U/mL penicillin and 50 µg/mL streptomycin) and aliquoted into 96-well plates, 180 µL per well. Stock solutions of each compound were prepared in dimethylsulfoxide (DMSO) and stepwise diluted in M199 media (Sigma). Growing concentrations of each compound (0.07–300 µM) were added to wells. The final concentration of DMSO was never higher than 0.1%. 20 µL of each prepared concentration were added for well. DMSO and AMBdc were included as negative and positive controls, respectively. All compounds and controls were assayed by triplicate.

2.4. Ex vivo splenic explant cultures

To obtain primary infected splenic explants, BALB/c mice were inoculated intraperitoneally with 10⁸ *L. infantum*-iRFP metacyclic promastigotes. Briefly, infective promastigotes were isolated from stationary-phase culture by negative selection with peanut agglutinin (Sigma) (Sacks and Perkins, 1984). Five weeks post-infection, mice were slaughtered and spleens were aseptically dissected, washed in cold phosphate-buffered saline (PBS), and placed in petri dishes. Small pieces were obtained by using a scalpel. In order to obtain a single-cell suspension, tissue was incubated with 5 mL of 2 mg/mL collagenase D (Roche) prepared in buffer (10 mM HEPES [pH 7.4], 150 mM NaCl, 5 mM KCl, 1 mM MgCl₂ and 1.8 mM CaCl₂) for 20 min. A cell suspension containing traces of spleen mass was gently passed through a 100-µm cell strainer to remove tissue fragments (Balaña-Fouce et al., 2012). Splenocytes were washed twice with PBS by centrifugation (500 × g for 7 min at 4 °C) and resuspended in RPMI medium supplemented with 10% FCS, 1 mM sodium pyruvate, 1 × RPMI vitamins, 10 mM HEPES, and 50 U/mL penicillin and 50 µg/mL streptomycin at 37 °C under a 5% CO₂ atmosphere. Cells were counted and diluted at different cell densities. Cells were seeded until confluence, and different concentrations of the studied compounds were administered to the explants for 48 h. The viability of infecting amastigotes was assessed by recording the fluorescence emission of infected splenocytes at 708 nm in an Odyssey (Li-Cor) infrared imaging system.

2.5. Cytotoxicity assay and selectivity index (SI) determination

Cytotoxicity of each compound was assessed on uninfected *ex vivo* explants and on the human hepatocarcinoma cell HepG2 line (ATCC HB-8065). HepG2 cells were cultured in The Glutmax Dulbecco's Modified Eagle's Medium (DMEM, Gibco), supplemented with 10% (v/v) FCS, 100 µg/mL penicillin and 100 µg/mL streptomycin. Both strains were seeded in 96-well plates in the presence of different concentrations of the assayed compound for 48 h at 37 °C. Viability of the cultures was determined using the Alamar Blue staining method, according to manufacturer's recommendations (Invitrogen).

Selectivity Indexes (SI) for the compounds were determined as the ratio between the CC₅₀ values for non-infected mouse splenocytes (SI_s) or CC₅₀ values for HepG2 (SI_h) and the EC₅₀ values for amastigotes in infected splenocytes.

2.6. Purification of leishmanial tubulin

L. infantum (wild type strain) tubulin was isolated according to (Yakovich et al., 2006). Two-liter flasks of *L. infantum* promastigotes were grown up to a cell density of approximately 1 × 10⁹ cells/mL. Cells were harvested and washed twice in PBS and resuspended in 0.1 mM piperazine N, N'-bis(2-ethanesulfonic acid) (PIPES) buffer (pH 6.9), containing 1 mM glycol ether diamine tetraacetic acid

(EGTA) and 1 mM MgCl₂. The resulting suspensions were sonicated on ice (5 cycles 5 pulses of 30 s each), and then were centrifuged in a Beckman Optima XL using a 70.1 Ti rotor at 40 000 × g for 45 min at 4 °C. The protein suspension was loaded onto a DEAE Sepharose (fast flow) and eluted with the same buffer containing 0.3 M KCl/0.75 M l-glutamate. The purity of the leishmanial tubulin suspension was more than 90% and was analyzed by polyacrylamide gel electrophoresis in denaturing conditions (SDS-PAGE).

2.7. Tubulin polymerization assays

Reactions of tubulin-assembly/depolymerization by drugs were carried out in 384-wells black microplates with optical bottom (Thermo) in a final volume of 40 µL. Each reaction contained 1.2 mg/mL freshly isolated *Leishmania* tubulin, 0.1 mM PIPES (pH 6.9), 1 mM EGTA and 1 mM MgCl₂, final concentrations, without or with the assayed compounds or colchicine as reference. The compounds were added to the microplate maintained at 4 °C. The assembly reaction was initiated by adding 2 µL of 40 mM GTP (2 mM final concentration). Variation of the absorbance at 340 nm was recorded in a Synergy HT microplate reader up to 45 min at 37 °C. IC₅₀ values are reported as the mean ± SD of at least three different experiments assayed by duplicate.

2.8. Molecular modelling and structural analysis

The homology model of *L. infantum* β-tubulin (GenBank LinJ.08.1280) was generated using the crystallographic structure of the bovine protein (PDB 4O2B) as template (Prota et al., 2014). An initial model was obtained with the SWISS-MODEL modelling server (Schwede et al., 2003) and the tools Modeller 9.13 (Sali and Blundell, 1993; Fiser et al., 2000; Marti-Remon et al., 2000). Molecular figures were prepared using VMD (Humphrey et al., 1996) and UCSF Chimera (Pettersen et al., 2004; Yang et al., 2012). The validation of the final model was carried out with MEAN (Benkert et al., 2008, 2009, 2011) and PROCHECK programs (Laskowski et al., 1993).

Molecular docking studies were carried out to identify the binding affinities between the inhibitors and tubulins. Docking calculations were performed using the AutoDock 4.2 software (Morris et al., 2009). A grid box of 66 × 44 × 66 points with a grid spacing of 0.375 Å and centered at the amino acid in position 200 was used to calculate the atom types needed for the calculations. The best binding mode of each molecule was selected based on the lowest binding free energy and the largest cluster. Ligand interactions with tubulin models of *Bos taurus* and *Leishmania* sp. were made with MAESTRO 10.2 software (Schrödinger, LLC, New York) using a 4 Å distance cut-off (http://platinhom.github.io/ManualHom/Schrödinger_2015_2_docs/maestro_user_manual.pdf)

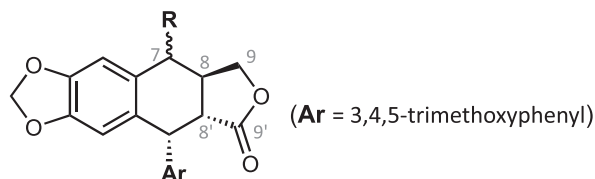
3. Results

3.1. Activity of podophyllotoxin derivatives against *L. infantum*

A set of 53 compounds with varied substitution arrangements on the fused tetracyclic core of podophyllotoxin or the tricyclic core of podophyllaldehyde (Fig. 1) were tested *in vitro* for their ability to kill both stages of *L. infantum*. Results from the antileishmanial tests revealed that some of these compounds killed both promastigotes and splenic amastigotes at low micromolar EC₅₀ level. Values of antiparasitic activity obtained with podophyllotoxin derivatives were generally better on intracellular amastigotes than on free-living promastigotes (Table 1). However, this result could be

Table 1

Structures and bioactivity results for podophyllotoxin derivatives. Antileishmanial effects ($EC_{50} \pm SD$) on promastigotes and amastigote-infected splenocytes (amastigotes) of *L. infantum*. Cytotoxicity effects ($CC_{50} \pm SD$) on murine splenocytes and human HepG2 hepatocytes. Inhibition effects ($IC_{50} \pm SD$) on leishmanial tubulin polymerization.



Comp.	R	EC_{50} (μM)		CC_{50} (μM)		IC_{50} (μM)		
		<i>L. infantum</i> promastigotes	<i>L. infantum</i> amastigotes	Murine Splenocytes	SI _S	Human HepG2	SI _h	<i>Leishmania</i> tubulin
1	H	>100	>100	98.6 \pm 3.1	<1.0	>100	un	7.9 \pm 0.3
2a		>100	13.4 \pm 0.8	>100	>7.4	0.7 \pm 0.0	0.1	0.3 \pm 0.0
2b		>100	>100	>100	<1.0	30.6 \pm 2.1	<0.3	2.7 \pm 0.1
3		>100	>100	60.6 \pm 7.7	<0.6	10.3 \pm 0.9	<0.1	4.0 \pm 0.2
4		23.2 \pm 0.5	>100	0.4 \pm 0.0	<0.01	>100	un	3.5 \pm 0.8
5a		13.8 \pm 0.2	15.6 \pm 0.1	16.4 \pm 1.7	1.1	>100	>6.4	1.1 \pm 0.1
5b		24.9 \pm 0.4	6.7 \pm 0.3	18.0 \pm 1.8	2.7	>100	> 14.9	5.0 \pm 0.3
6a		>100	7.4 \pm 0.4	6.4 \pm 0.8	0.9	33.1 \pm 2.1	4.5	3.4 \pm 0.3
6b		14.5 \pm 0.3	9.3 \pm 0.4	1.7 \pm 0.2	0.2	>100	> 10.8	4.1 \pm 0.1
7^a		10.4 \pm 0.6	44.3 \pm 3.2	6.8 \pm 0.2	0.2	>100	>2.3	7.7 \pm 0.6
8		61.2 \pm 7.8	>100	55.5 \pm 3.3	<0.6	76.0 \pm 1.5	<0.8	8.0 \pm 1.4
9		>100	53.7 \pm 5.2	57.1 \pm 2.5	1.1	>100	>1.9	6.9 \pm 0.5
10		>100	46.3 \pm 8.8	15.9 \pm 0.1	0.3	>100	>2.2	4.4 \pm 0.9
11		>100	79.1 \pm 5.3	38.0 \pm 2.5	0.5	>100	>1.3	8.8 \pm 4.5
12		66.4 \pm 6.8	>100	11.4 \pm 2.0	0.1	>100	un	3.4 \pm 0.5
13		>100	5.9 \pm 1.1	4.3 \pm 0.6	0.7	>100	> 17.1	5.5 \pm 0.0
Miltefosine		5.9 \pm 1.4	2.40 \pm 0.2	64.7 \pm 7.0	26.9	50.4 \pm 4.3	21	nt
AMBdc		0.8 \pm 0.1	0.3 \pm 0.0	>20	>62.5	nt	un	nt

^a -1:1 mixture of C-7 α and C-7 β epimers. SI_S: Selectivity Index (mouse splenocytes); SI_h: Selectivity Index (human HepG2); nt: not tested; un: undefined. Significant values (EC_{50} : <10 μM , SI: > 10, and IC_{50} : <1 μM) are **bolded** for comparison purposes.

due to the close values found for anti-amastigote activity of the compounds and their cytotoxicity for uninfected host macrophages.

We examined the EC_{50} values found for podophyllotoxins with antileishmanial effect against amastigotes in the context of

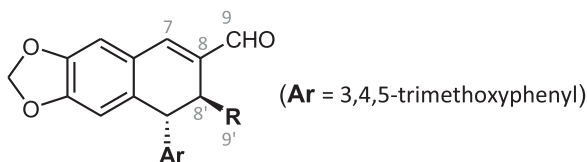
molecular structure-activity correlation. An initial comparison revealed that while the unsubstituted core molecule deoxy-podophyllotoxin (**1**) was essentially inactive (EC_{50} > 100 μM), the presence of a single hydroxyl (OH) substituent at C-7 α in podophyllotoxin (**2a**) conferred a significant antileishmanial activity

(EC₅₀: 13.4 μM). Similarly, the presence of small aliphatic alkyl or alkenyl substituents at position C-7 (compounds **4–6b**), did increase substantially the killing potency of the parental compound **1** on both *Leishmania* and mouse cells, while lesser or minimum enhancements were observed after the introduction of larger alkenyl (**7, 8**), or hydroxyalkyl (**9, 10**), or alkoxy/cycloalkoxy (**11, 12**) substituents. Very interestingly, the presence of a 7α-pyranylglycol fragment in compound **13**, led to the most potent antiamastigote molecule of this series. Though the antileishmanial potency of several compounds of this series resulted in the range of the clinically used antimonial drugs and miltefosine (Seifert et al., 2003;

Mandal et al., 2015), none of the compounds assayed attained the leishmanicidal potency of AMBdc (EC₅₀: 0.3 μM), which is currently the most potent reference drug in these assays.

To provide a uniform basis for comparison in these studies, we assayed all the compounds listed in Tables 1–4 against mouse spleen macrophages – a primary non-tumoral culture, that represents the benchmark for comparative screening of antileishmanial drug candidates– and on HepG2 hepatocytes, a human model for studies of liver drug toxicity. Although most compounds were less toxic for human hepatocytes, only two out from those 16 tested were fairly more potent against *Leishmania* amastigotes than

Table 2
Structures and bioactivity results for podophyllic aldehyde derivatives with changes at the C9'-side chain R. Antileishmanial effects (EC₅₀ ± SD) on promastigotes and amastigote-infected splenocytes (amastigotes) of *L. infantum*. Cytotoxicity effects (CC₅₀ ± SD) on murine splenocytes and human HepG2 hepatocytes. Inhibition effects (IC₅₀ ± SD) on leishmanial tubulin polymerization.

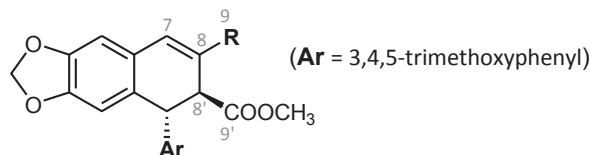


Comp.	R	EC ₅₀ (μM)		CC ₅₀ (μM)		IC ₅₀ (μM)		
		<i>L. infantum</i> promastigotes	<i>L. infantum</i> amastigotes	Murine Splenocytes	SI _s	Human HepG2	SI _h	<i>Leishmania</i> tubulin
14	COOCH ₃	89.5 ± 4.3	9.3 ± 0.5	>100	> 10.8	>100	> 10.8	2.0 ± 0.3
15	COOCH=CH ₂	57.0 ± 4.2	29.8 ± 1.6	>100	>3.3	>100	>3.3	0.7 ± 0.0
16	COO(CH ₂) ₃ Br	35.2 ± 7.5	nt	98.2 ± 10.2	un	nt	un	1.7 ± 0.1
17	COO(CH ₂) ₆ Br	25.7 ± 3.6	18.1 ± 0.1	46.8 ± 7.0	2.6	68.9 ± 6.0	3.8	7.0 ± 0.7
18	COOCH ₂ COOCH ₂ CH ₃	64.8 ± 4.9	4.3 ± 0.1	>100	> 23.4	10.4 ± 0.8	2.4	0.9 ± 0.1
19		>100	56.3 ± 1.4	42.0 ± 1.9	0.7	73.5 ± 11.6	1.3	>20
20		17.5 ± 0.9	20.9 ± 0.1	21.0 ± 2.3	1.0	45.5 ± 5.6	2.2	4.3 ± 0.4
21		79.9 ± 5.7	51.9 ± 0.3	34.1 ± 3.5	0.7	18.5 ± 0.7	0.4	2.0 ± 0.0
22	COOCH ₂ Ar	14.5 ± 1.1	10.2 ± 0.5	51.3 ± 3.0	5.0	89.9 ± 4.0	8.8	3.1 ± 0.2
23		9.3 ± 0.7	9.9 ± 0.5	>100	> 10.0	>100	> 10.0	0.8 ± 0.0
24		94.8 ± 7.9	>100	>100	un	14.3 ± 1.2	un	>20
25^a		>100	>100	>100	un	>100	un	>20
26		>100	>100	80.1 ± 4.9	<0.80	27.2 ± 2.2	0.27	>20
Miltefosine		5.9 ± 1.4	2.4 ± 0.2	64.7 ± 7.0	26.9	50.4 ± 4.3	21	nt
AMBdc		0.8 ± 0.1	0.3 ± 0.0	>20	> 62.5	nt	un	nt

^a Complete structure of this compound. SI_s: Selectivity Index (splenocytes); SI_h: Selectivity Index (HepG2); nt: not tested; un: undefined. Significant values (EC₅₀: ≤ 10 μM, SI: ≥ 10, and IC₅₀: ≤ 1 μM) are **bolded** for comparison purposes.

Table 3

Structures and bioactivity results for podophyllic aldehyde derivatives with modifications at position C-9. Antileishmanial effects ($EC_{50} \pm SD$) on promastigotes and amastigote-infected splenocytes (amastigotes) of *L. infantum*. Cytotoxicity effects ($CC_{50} \pm SD$) on murine splenocytes and human HepG2 hepatocytes. Inhibition ($IC_{50} \pm SD$) of leishmanial tubulin polymerization.



Comp.	R	EC_{50} (μM)		CC_{50} (μM)		IC_{50} (μM)		
		<i>L. infantum</i> promastigotes	<i>L. infantum</i> amastigotes	Murine Splenocytes	SI_s	Human HepG2	SI_h	<i>Leishmania</i> tubulin
27		38.3 \pm 3.7	31.7 \pm 2.1	>100	>6.3	6.6 \pm 0.4	0.2	12.1 \pm 0.8
28		24.5 \pm 1.5	24.5 \pm 1.5	>100	>4.1	>100	>4.1	2.9 \pm 0.3
29		61.3 \pm 0.7	59.4 \pm 0.8	>100	>1.7	>100	>1.7	>20
30		19.9 \pm 2.1	19.9 \pm 2.1	>100	>5.1	nt	un	5.6 \pm 0.5
31		9.4 \pm 0.7	9.4 \pm 0.7	>100	>10.1	1.1 \pm 0.0	0.1	1.2 \pm 0.1
32		14.2 \pm 1.8	53.4 \pm 4.5	79.3 \pm 7.9	1.5	nt	un	>20
33		41.1 \pm 2.4	70.5 \pm 3.7	38.7 \pm 1.5	0.5	>100	1.4	4.3 \pm 0.6
34		94.5 \pm 3.0	15.6 \pm 0.8	>100	>6.4	1.5 \pm 0.1	0.1	0.8 \pm 0.0
35		91.0 \pm 2.0	67.4 \pm 2.0	>100	>1.5	32.4 \pm 0.6	0.5	1.6 \pm 0.2
36		51.6 \pm 1.8	7.5 \pm 0.5	58.1 \pm 2.7	7.7	nt	un	9.0 \pm 0.8
37		14.2 \pm 2.1	25.3 \pm 1.0	8.8 \pm 0.5	0.3	>100	>3.9	7.5 \pm 1.1
38		>100	>100	>100	un	>100	un	>20
39		45.2 \pm 2.8	24.3 \pm 0.5	22.9 \pm 0.9	0.9	87.3 \pm 6.4	3.6	3.1 \pm 0.2
Miltefosine		5.9 \pm 1.4	2.4 \pm 0.2	64.7 \pm 7.0	26.9	50.4 \pm 4.3	21.0	nt
AMBdc		0.8 \pm 0.1	0.3 \pm 0.0	>20	> 62.5	nt	un	nt

SIS: Selectivity Index (splenocytes), SI_h: Selectivity Index (HepG2), nt: not tested, un: undefined. Significant values (EC_{50} : <10 μM , SI: > 10, and IC_{50} : <1 μM) are **bolded** for comparison purposes.

cytotoxic for uninfected splenocytes. The highest selectivity indexes (SI_s) for amastigotes were found for podophyllotoxin (**2a**, $SI_s > 7.4$) and the isobutyl derivative **5b**, which displayed a modest $SI_s = 2.7$. The remaining compounds had $SI_s \leq 1.1$ (similarly toxicity for both cell lines or even more toxic for the host cell) and therefore, they were not considered as candidates for further experiments.

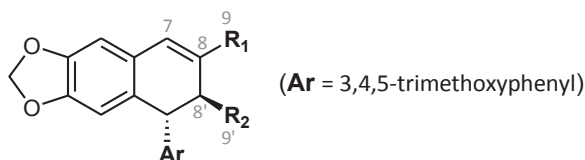
The glycolic podolignan **13**, though practically inactive against promastigotes and highly cytotoxic for mouse splenocytes, was the most potent molecule of this series against amastigotes, and also turned out to be the most selective with respect to human hepatocytes ($SI_h > 17.1$). These facts suggest the potential interest of

extending the antileishmanial evaluation to other podolignans containing such a glycolic fragment attached to the C-7 position.

3.2. Activity of podophyllic aldehyde derivatives against *L. infantum*

In a second instance, the antileishmanial activity of three series of compounds derived from podophyllic aldehyde (**14**) was evaluated. This aldehyde was considered as a potential antiparasitic lead compound, due to its selectivity previously shown against cancer vs normal cells (Gordaliza et al., 2000). The aldehyde **14** is a cyclo-lignan resulting from a multi-step chemical process around the

Table 4
Structures and bioactivity results for lignan-heterocycle hybrids with modifications at C-9. Antileishmanial effects ($EC_{50} \pm SD$) on promastigotes and amastigote-infected splenocytes (amastigotes) of *L. infantum*. Cytotoxicity effects ($CC_{50} \pm SD$) on murine splenocytes and human HepG2 hepatocytes. Inhibition ($IC_{50} \pm SD$) of leishmanial tubulin polymerization.



Comp.	R ₁	R ₂	EC ₅₀ (μM)		CC ₅₀ (μM)		IC ₅₀ (μM)		
			<i>L. infantum</i> promastigotes	<i>L. infantum</i> amastigotes	Murine Splenocytes	SI _s	Human HepG2	SI _h	<i>Leishmania</i> tubulin
40		COOCH ₃	19.4 ± 2.1	4.5 ± 0.1	>100	> 22.2	8.8 ± 0.3	2.0	1.51 ± 0.0
41		COOCH ₃	16.3 ± 1.9	9.7 ± 1.8	86.2 ± 0.1	8.9	nt	un	16.1 ± 2.1
42		COOCH ₃	13.9 ± 2.8	12.1 ± 0.4	>100	>8.4	46.8 ± 1.3	3.9	12.1 ± 1.2
43		COOCH ₃	>100	99.4 ± 6.3	15.6 ± 0.6	0.2	47.5 ± 0.3	0.5	>20
44		COOCH ₃	>100	42.3 ± 3.1	>100	>2.4	>100	>2.4	>20
45		COOCH ₂ CH ₃	16.1 ± 2.2	2.5 ± 0.2	71.8 ± 6.0	29.0	nt	un	>20
46		COOCH ₃	34.3 ± 1.7	7.3 ± 0.2	>100	> 13.7	51.2 ± 3.6	7.0	0.7 ± 0.0
47		COOCH ₃	>100	2.2 ± 0.3	>100	> 45.5	9.9 ± 0.6	4.4	>20
48		COOCH ₃	11.0 ± 0.7	8.9 ± 0.6	71.0 ± 1.5	8.0	65.9 ± 3.3	7.4	1.3 ± 0.0
49		COOCH ₃	47.0 ± 5.2	21.2 ± 1.1	40.7 ± 6.5	1.9	95.0 ± 14.0	4.5	0.3 ± 0.0
50		COOCH ₃	>100	43.4 ± 2.1	53.3 ± 3.5	1.2	92.5 ± 6.8	2.1	>20
Miltefosine			5.9 ± 1.4	2.4 ± 0.2	64.7 ± 7.0	26.9	50.4 ± 4.3	21.0	nt
AMBdc			0.8 ± 0.1	0.3 ± 0.0	>20	> 62.5	nt	un	nt

SI_s: Selectivity Index (splenocytes), SI_h: Selectivity Index (HepG2), nt: not tested, un: undefined, Significant values (EC_{50} : <10 μM, SI: > 10, and IC_{50} : <1 μM) are **bolded** for comparison purposes.

fused γ -lactone ring of podophyllotoxin (including D-ring lactone rupture with C-8' epimerization and C-9' esterification, C7-C8 dehydration and C-9 oxidation), finally leading to the C9-aldehyde function and the β -axially-oriented carboxylic methyl ester at C-9'. Many compounds of the first series of podophyllin derivatives (**14–24**), retained the aldehyde function at C-9 in order to investigate the influence of nature and size of the ester chain at position C-9' upon the antileishmanial activity and cytotoxicities (Table 2). Additionally, the series includes one compound with the common trimethoxyphenyl (Ar) fragment extended to a methoxyphthalazine moiety (**25**) and a pyrrolidide (**26**). These are representatives of two available sub-series of compounds, aiming to detect the respective and possible influence on the activity by enlarging the polycyclic structure, and by changing from the ester to an amide function at position C-9'.

As in the case of podophyllotoxin derivatives, though with the exceptions of the chloropurine derivative **20** and the

pseudodimeric diester **24**, the antileishmanial potency of those active C9'-esters was generally higher (comps. **14**, **15**, **17–19**, **21** and **22**) against the amastigote form of the parasite, or similar (**23–26**) against both forms. The virtual inactivity observed for the phthalazine **25** and the pyrrolidide **26** led to preclude further evaluation of their related sub-series of analogues.

Interestingly, related to the antiparasitic selectivity within this series (Table 2), the starting lead compound, the aldehyde **14**, and two of its more potent derivatives, the glycolate ester **18** and the cinnamyl ester **23**, displayed significant SI_s values of SI_s > 10.8, >23.4 and > 10.0 respectively, although the derivative **18** showed higher cytotoxicity for HepG2 hepatocytes (SI_h = 2.4). On the contrary, the trimethoxybenzyl ester **22** provided low hepatocyte toxicity (CC₅₀: 89.9 μM), but less significant SI_s values (SI_s = 5.0). In addition, the presence of a terminal olefin, the allyl ester **15** behaved in a similar way (SI_s > 3.3). For other compounds of the series, the actual EC₅₀ values were compromised with their

respective CC_{50} and with splenocytes survival.

The second series of podophyllaldehyde derivatives (Table 3), included those compounds resulting from the reaction of the aldehyde (-CHO) group at position C-9 with a number of amine, hydrazine and hydroxylamine reagents, thus leading to a diversity of compounds, including the saturated amine **27**, the hydrazone **28**, the oxime **29**, the monoimines **30–37**, the symmetric azine **38** and the di-imine **39**. The compounds were evaluated on both stages of *L. infantum* and, as expected (Table 3), the nature and size of the imine substituents influenced their leishmanicidal activity. It should be noted that compounds with the imino C9=N double bond may decompose during the assays and, consequently, would act as pro-drugs of the starting podophyllaldehyde. This could particularly happen in the case of *in vivo* or prolonged *in vitro* assaying, due to their possible metabolic or chemical hydrolysis, with simultaneous liberation of the corresponding amine.

Unlike the majority of molecules so far tested, a moderate but significant SI_s was found for most of compounds belonging of this series. The most potent compounds of this group in killing *L. infantum* amastigotes were the thiazolyl-imine **36** ($EC_{50} = 7.5 \mu\text{M}$), and the phenolic-imine **31** ($EC_{50} = 9.4 \mu\text{M}$), which also displayed the highest SI_s values (7.7 and > 10.1 , respectively). The remaining compounds had lower potency and more modest selectivities. It should be also noted the potential hepatotoxicity of this series of compounds, with the trifluoroethylhydrazone **28**, as the only member showing a SI_h value higher than 4. However, some attention should be paid to the saturated amine **27** ($SI_s > 6.3$), because despite its discrete leishmanicidal potency ($EC_{50} = 31.7 \mu\text{M}$) and its certain hepatotoxicity ($SI_h = 0.2$), it was unable to destroy murine splenocytes at the maximum concentration tested of $100 \mu\text{M}$. This would be chemically supported by the less reactive character of amines with respect to the unsaturated imines, oximes and hydrazones. This would suggest to extend the leishmanicidal and cytotoxicity evaluations to other saturated analogues, with other secondary or tertiary amine functions attached to C-9. Furthermore, from the chemical and pharmacological mechanistic points of view, the amines would act by themselves rather than as pro-drugs, as they are more stable than those unsaturated derivatives and should need a harder metabolic processing of oxidative deamination to liberate the precursor podophyllaldehyde **14**.

Finally, Table 4 shows the structures and antileishmanial results of the third series of podophyllaldehyde derivatives **40–50**. All these compounds contain a bicyclic heterocyclic system built on the aldehyde function and integrating the C-9 carbon atom of the lignan into the heterocyclic fragment. The added fragments were structurally close to nucleic purine bases, benzoxazole, benzimidazole and benzothiazole systems, which are fragments often present in many antiparasitic and antimicrobial agents. In general, as in the above series, these hybrid compounds were more effective in killing intracellular amastigotes than against promastigotes of *L. infantum*. Interestingly, more than the half of the tested compounds of this series had EC_{50} values below $20 \mu\text{M}$, being the benzimidazole derivatives **45** ($EC_{50} = 2.5 \mu\text{M}$) and **47** ($EC_{50} = 2.2 \mu\text{M}$) that presented the highest and similar antileishmanial potencies. The cytotoxicity of these compounds, was also assayed on murine splenocytes. Most interestingly, these lignan-benzimidazole/benzoxazole hybrids were revealed as very selective against amastigote-infected splenocytes, with high values for the lignan-benzimidazole hybrids **47** ($SI_s > 45.5$), **45** ($SI_s = 29.0$) and **46** ($SI_s = > 13.7$), and significant values for the lignan-benzoxazole hybrids **40** ($SI_s > 22.2$), **41** ($SI_s = 8.9$), **42** ($SI_s > 8.4$) and the dichlorobenzimidazole **48** ($SI_s = 8.0$). Unfortunately, cytotoxicities for human HepG2 hepatocytes were not so good and only the compounds **46** and **48** displayed good SI_h values of 7.0 and 7.4,

respectively.

3.3. Inhibition of tubulin polymerization

The entire list of compounds was assayed on freshly purified tubulin obtained from *L. infantum* promastigotes as described above (see Fig. S1 A and B from Supplementary Material). Firstly, the compounds were tested at a single concentration of $20 \mu\text{M}$ to discard less potent substances. Then, those active inhibitors of tubulin polymerization were tested at different concentrations to determine their IC_{50} values (results shown in Tables 1–4). Podophyllotoxin (**2a**) and podophyllaldehyde (**14**) were used for comparison purposes within their respective series 1 and 2–4. Vinblastine, that inhibits completely tubulin polymerization at $25 \mu\text{M}$ concentration, was used as positive control in the assay.

As expected, a relevant number of compounds, including podophyllotoxin (**2a**) and six podophyllaldehyde derivatives (**15**, **18**, **23**, **34**, **46** and **49**) showed IC_{50} values under the μM level, while other 20 compounds ranged between 1 and $5 \mu\text{M}$. The most effective inhibitors of Leishmania tubulin polymerization were the lignan-imidazopyridine hybrid **49** ($IC_{50} = 310 \text{ nM}$) and the lignan-benzimidazole hybrid **46** ($IC_{50} = 660 \text{ nM}$), both in the range of potency of podophyllotoxin (**2a**, $IC_{50} = 320 \text{ nM}$) and fairly more potent than podophyllaldehyde (**14**, $IC_{50} = 2.0 \mu\text{M}$) (see Fig. S2 from Supplementary Material). Surprisingly, the antileishmanial and the antitubulin results did not fully correlate. The most potent anti-tubulin, the imidazopyridine hybrid **49**, had resulted less potent (EC_{50} : $21.2 \mu\text{M}$) and fairly less selective (SI_s : 1.9) antileishmanial than the above-mentioned benzimidazole (SI_s : 8.0–45.5) and benzoxazole (SI_s : > 8.4 –22.2) hybrids.

3.4. Molecular modelling

The colchicine-binding site lies at the interface between the α and β subunits of the tubulin heterodimer (Fig. 2A and B). Three interaction zones in the β subunit (zones 1, 2 and 3) have been identified in the mammalian model (Massarotti et al., 2012). Both colchicine and podophyllotoxin interact with amino acids of the α subunit and with those near the interface of zone 2 in the β heterodimer. Amino acids involved in the interaction with colchicine in the α subunit are fully conserved without any remarkable polymorphism in *Leishmania*. However, several non-synonymous mutations of *Leishmania* β tubulin may be responsible for the lack of activity of colchicine in trypanosomatids. Amongst them, $^{259}\text{Met} \rightarrow ^{259}\text{Leu}$; $^{316}\text{Ala} \rightarrow ^{316}\text{Ser}$ and $^{354}\text{Ala} \rightarrow ^{354}\text{Ser}$ (Fig. 2C) are involved in the interaction with the trimethoxybenzene fragment of colchicine, and would be responsible for its difficult conformational arrangement into the binding site. These and other site changes are responsible for the constrained volume of colchicine binding site in leishmanial tubulin (from 726.6 \AA^3 in mammals to 696.0 \AA^3 in *Leishmania*), and should explain why colchicine is unable to interact favorably with its own leishmanial binding site (Fig. 2D and E).

A modelling study of the β subunit of *Leishmania* tubulin was conducted on the basis of an interaction complex model of calf tubulin with podophyllotoxin (PDB:4O2B) [30]. For this purpose, the co-crystal model of calf tubulin-colchicine complex was used as template for *Leishmania* tubulin modelling, using the AutoDockTools program. Interactions between podophyllotoxin analogues with calf and *Leishmania* tubulins were calculated with AUTODOCK. Apparently, most of the compounds bind tightly to *Leishmania* tubulin (Table 5), although some compounds interact with calf tubulin with higher affinity than with *Leishmania* tubulin. This may be due to the actual conformations adopted by different podolignans in their respective interactions with calf or leishmanial β -tubulins.

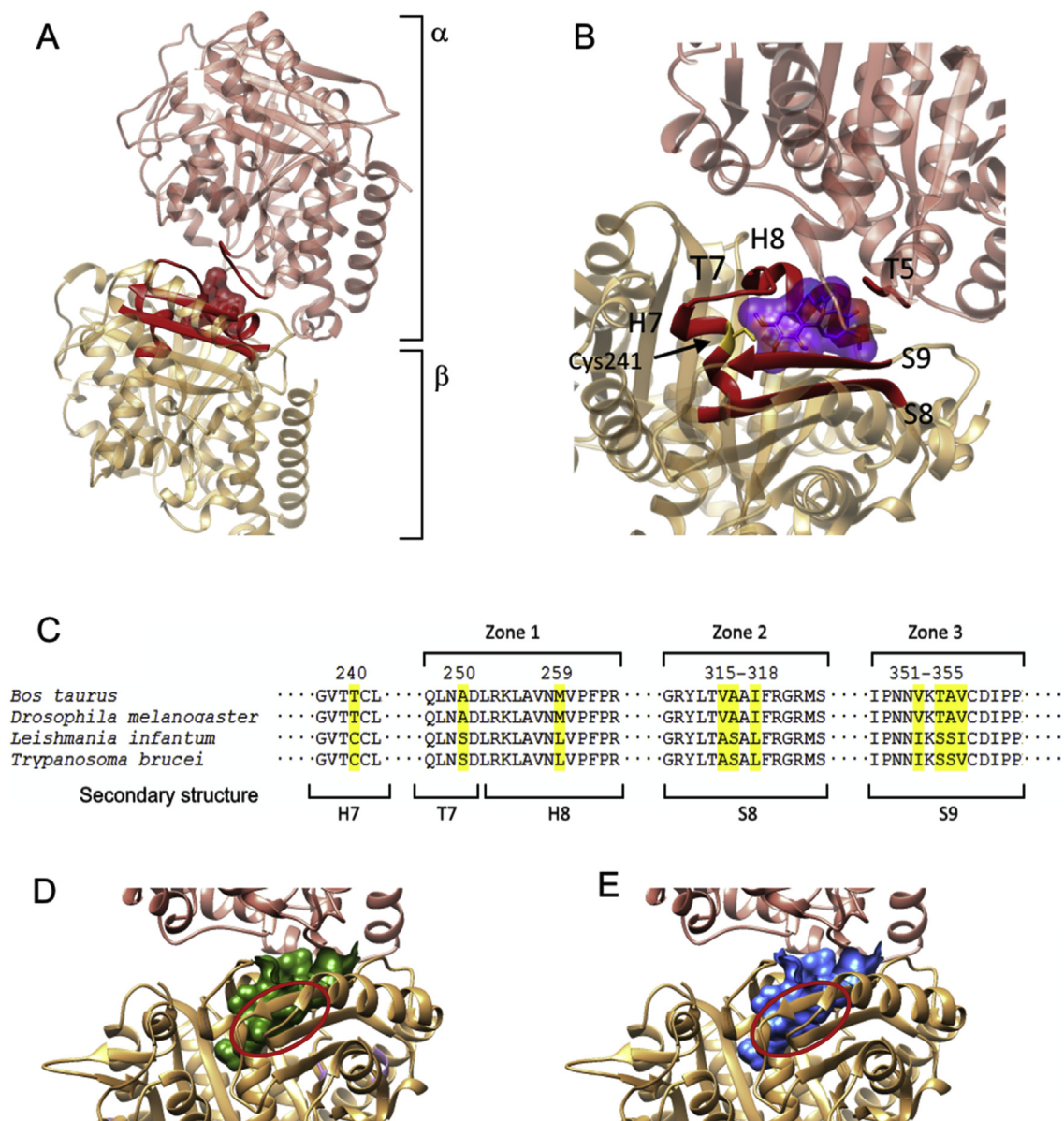


Fig. 2. (A) Ribbon 3D diagram of α and β subunits of *L. infantum* tubulin dimer. The homology model was generated by superimposition of the structure generated with the α/β -tubulins from *L. infantum* (GenBank LinJ.13.0330 and LinJ.08.1280) using the crystallographic structure of the bovine protein with colchicine (PDB:4O2B) as template [30]. (B) Structural motifs of calf α/β tubulin involved in colchicine binding site. Colchicine (violet) is bound to domains and secondary structure elements of both subunits. In the α -tubulin, amino acids associated with the T5 loop form part of the pocket-binding site. Elements of β -tubulin are presented and defined as follows: α -helices H7–8, β sheets 8–9 and T7 loop. (C) Multiple alignment of the peptide sequence of the β subunit of tubulin *B. taurus*, *Saccharomyces cerevisiae*, *L. infantum* and *Trypanosoma brucei* involved in the colchicine binding site, showing the pointed polymorphisms in yellow. Representation of a tubulin dimer with the colchicine binding pocket surface in *B. taurus* (D) and *L. infantum* (E). (For interpretation of the references to colour in this figure legend, the reader is referred to the web version of this article.)

To analyze such conformational differences in the interaction complexes, podophyllotoxin (**2a**), podophyllic aldehyde (**14**) and two derivatives with strong antitubulin effect (**46** and **49**) were submitted to a conformational force field optimization implemented by ChemDraw 3D, and docked into leishmanial and calf tubulins. Fig. 3 (left columns) shows that the docking of podolignans within the pocket-binding site of *Leishmania* tubulin can be different enough (**2a**, **46**, **49**) from those found in mammal tubulin (right column), while other (**14**) results close similar.

The key interactions between the selected compounds and their corresponding amino acids in the colchicine-site of *Leishmania* and calf tubulins are described in the 2D interaction maps included in Fig. 4 (See also other 2D maps in Fig. S3, of supplementary

material). Most amino acids involved in the interaction of podophyllotoxin with β -tubulin in calf are conserved in the *Leishmania* model. However, several changes alter the conformational disposition of the drug within the pocket-binding site of the parasite protein. Looking at 2D maps of podophyllotoxin (**2a**), the change of ²⁵⁹Met \rightarrow ²⁵⁹Leu in the zone 1 (Fig. 3C) of *Leishmania* β -tubulin alters deeply the disposition of the tetracyclic core of podophyllotoxin in *Leishmania*. The dioxole ring of **2a**, surrounded by the amino acids ²⁵⁸Asn in zone 1 and ³¹⁴Thr and ³¹⁵Val of zone 2 in calf tubulin, is exposed to solvent in the *Leishmania* model due to a 180° rotation of the molecule. However, the trimethoxyphenyl group is not exposed to solvent in this model due to the ²⁵⁰Ala \rightarrow ²⁵⁰Ser change in zone 1 and ³¹⁶Ala \rightarrow ³¹⁶Ser change in zone 2. These

Table 5
Tubulin polymerization inhibition, docking energy values and correlative data for representative lignans and hybrid compounds of this research.

Compd.	<i>Leishmania</i> tubulin polymerization inhibition (IC ₅₀ μM)	Docking energy <i>Leishmania</i> (kcal/mol)	Docking energy <i>Bos taurus</i> (kcal/mol)
2a	0.32 ± 0.03	−9.0	−8.0
5a	1.14 ± 0.14	−8.9	−7.7
14	2.05 ± 0.32	−7.5	−7.4
15	0.75 ± 0.04	−7.9	−7.9
21	2.02 ± 0.02	−7.4	−7.4
23	9.92 ± 0.55	−10.2	−7.9
31	1.16 ± 0.06	−8.4	−8.8
34	0.78 ± 0.04	−7.8	−9.1
35	1.64 ± 0.18	−8.5	−8.4
40	1.51 ± 0.05	−8.3	−8.3
46	0.66 ± 0.01	−8.4	−10.3
48	1.32 ± 0.01	−9.8	−7.1
49	0.31 ± 0.01	−9.2	−10.3
Colchicine	>100	df	−10.3

df: docking failure.

changes can also explain the improved interaction of podophyllotoxin with *Leishmania* β-tubulin in terms of a better docking energy (−9.0 kcal/mol in leishmanial vs −8.0 kcal/mol in mammalian tubulins; Table 5). Looking at the interaction complexes (Fig. 3), 2D maps (Fig. 4) and docking energies (Table 5) of the hybrid compounds **46** and **49**, more important conformational and docking energy differences can be observed. Obviously, such differences are due to the bicyclic heterocyclic fragments attached to the lignan and their bulkier structures, in comparison with those in **2a** and **14**. Similar studies have been carried out with other compounds included in Table 5 and graphic results and data can be found in supplementary files (Fig.S3 and Table S1).

4. Discussion

Despite the phylogenetic conservation of α- and β-tubulins, subtle structural differences in the tubulin-binding site for certain antitubulin compounds in kinetoplastids have suggested these proteins as a potential druggable target. Specifically, colchicine is a potent antimetabolic drug that has given rise to lots of new compounds, including podophyllotoxin derivatives and combretastatin A4 analogues, some of them under clinical trials (Kaur et al., 2014). From the comparison of 3D models of calf and *Leishmania* β-tubulins, the colchicine-binding site of the β-heterodimer is specially enriched in amino acid polymorphisms, which reduce the volume of this binding site in *L. infantum* (Fig. 2D and E). In addition to the constrained volume, another reason to explain the lack of effect of colchicine can be found in the modification of hydrophobicity in the binding site. From the 3D model shown in Fig. 2B (and embedded table) the colchicine-binding site lies between the α and β subunits. It consists of two S8 and S9 sheets, two H7 and H8 helices connected by the T7 hinge, and the T5 loop at the α-tubulin subunit. H7 helix contains the ²⁴¹Cys, which interacts with the conformationally restricted trimethoxybenzene moiety present in colchicine and with the more flexible trimethoxyphenyl group of podophyllotoxin derivatives. According to this model it can be suggested that the substitution of ²⁵⁹Met from zone 1 (comprised by T7 loop and H8 helix) of calf β-tubulin by a ²⁵⁹Leu may contribute to the significant displacement of planar R1 pharmacophore (A to D rings) of podophyllotoxin within the Leishmanial binding pocket. To this spatial change, the existence of three non-synonymous mutations within zones 1, 2 and 3 (²⁵⁰Ala → ²⁵⁰Ser, ³¹⁶Ala → ³¹⁶Ser and ³⁵⁴Ala → ³⁵⁴Ser) can generate some hydrophobicity reductions

in several parts of the *Leishmania* binding pocket. Many of those amino acids that have been changed should be involved in van der Waals (Ala)/polar (Ser) interactions with the conformationally rigid colchicine molecule, and also with combretastatins and podophyllotoxins, through their at least partially rotatable trimethoxyphenyl ring (ter Haar et al., 1996).

In other sense, the analysis of the effects of podophyllotoxin derivatives has shown that the hydroxyl group at position C-7α was essentially needed for the antileishmanial effect. Lack or change of the substituent at such position and orientation, represented by deoxypodophyllotoxin (**1**), the 7-epimer epipodophyllotoxin (**2b**) and the keto derivative podophyllotoxone (**3**), led to ineffective killers of *Leishmania* parasites with much lower effects in preventing tubulin polymerization (López-Pérez et al., 2004).

Here, we also found that there was no improvement in the polymerization inhibition of leishmanial tubulin with compounds having other substituents at positions C-7α or C-7β. This decrease in activity was previously observed on other cell lines, (Castro et al., 2003; López-Pérez et al., 2004; Abad et al., 2012), and could be due to additional spatial hindering for the binding to tubulin. However, relevant exceptions of highly potent polymerization inhibition of mammalian tubulin were demonstrated for some 7α-alkyl and 7α-hydroxycycloalkyl derivatives, as for 7α-isopropyl derivative **4** and for the glycolic pyranil derivative **13** (Abad et al., 2012) included in this research (Table 1).

It was also demonstrated that many podophyllaldehyde derivatives had interesting antileishmanial activity, with SI values higher than those provided by podophyllotoxin. Modelling of podophyllaldehyde (**14**, Figs. 3 and 4) shows a pattern of interaction similar to podophyllotoxin at the colchicine site of leishmanial tubulin. In this case, the ε-amino group of ²⁵⁴Lys (Fig. 4/14) in zone 1 of *L. infantum* β-tubulin is close enough to interact with the C9-carbonyl group of podophyllaldehyde, while ²⁴⁷Gln may interact with the dioxolic ring A. On the other hand, the trimethoxyphenyl fragment would undergo some interaction disturbances due to the presence of ²⁵⁰Ser, ³¹⁶Ser and ³¹⁸Leu in *Leishmania* tubulin, with respect to those of ²⁵⁰Ala, ³¹⁶Ala and ³¹⁸Ile in bovine tubulin.

For the series of compounds with the C9-aldehyde group integrated into a bicyclic heterostructure and the β-carboxyester function at C-9', we observed that some of them displayed more potent antileishmanial effects, also with good SI values for infected splenocytes. In general, these hybrid compounds showed better results in terms of potency than those from the other series, and can be compared well with those for glucantime and miltefosine (Seifert et al., 2003; Mandal et al., 2015), although they were less effective than AMBdc. Concerning the inhibitory action on leishmanial tubulin, the hybrid benzoxazole **40**, the benzimidazoles **46** and **48** and the imidazopyridine **49** inhibited its polymerization at low μM levels or even below micromolar concentrations. The benzoxazole **40** had a strong antitubulin effect (IC₅₀; 1.51 μM) in parallel with its high antileishmanial potency and selectivity (SI_s > 22.2). However, the dimethylbenzimidazole **47**, which displayed a higher antileishmanial potency and the highest selectivity (SI_s > 45.5) of all the compounds tested, did not show good inhibitory activity (IC₅₀ > 20 μM) on tubulin polymerization. It is worth mentioning here that benzimidazole and benzothiazole compounds are well-known inhibitors of tubulin polymerization in nematodes. Several efforts to find correlations between antileishmanial and/or antitubulin effects with docking energies for the compounds included in Table 5 were unsuccessful. These facts suggest the probable existence of an alternative mechanism of action for a number of compounds that need to be studied and established through further research.

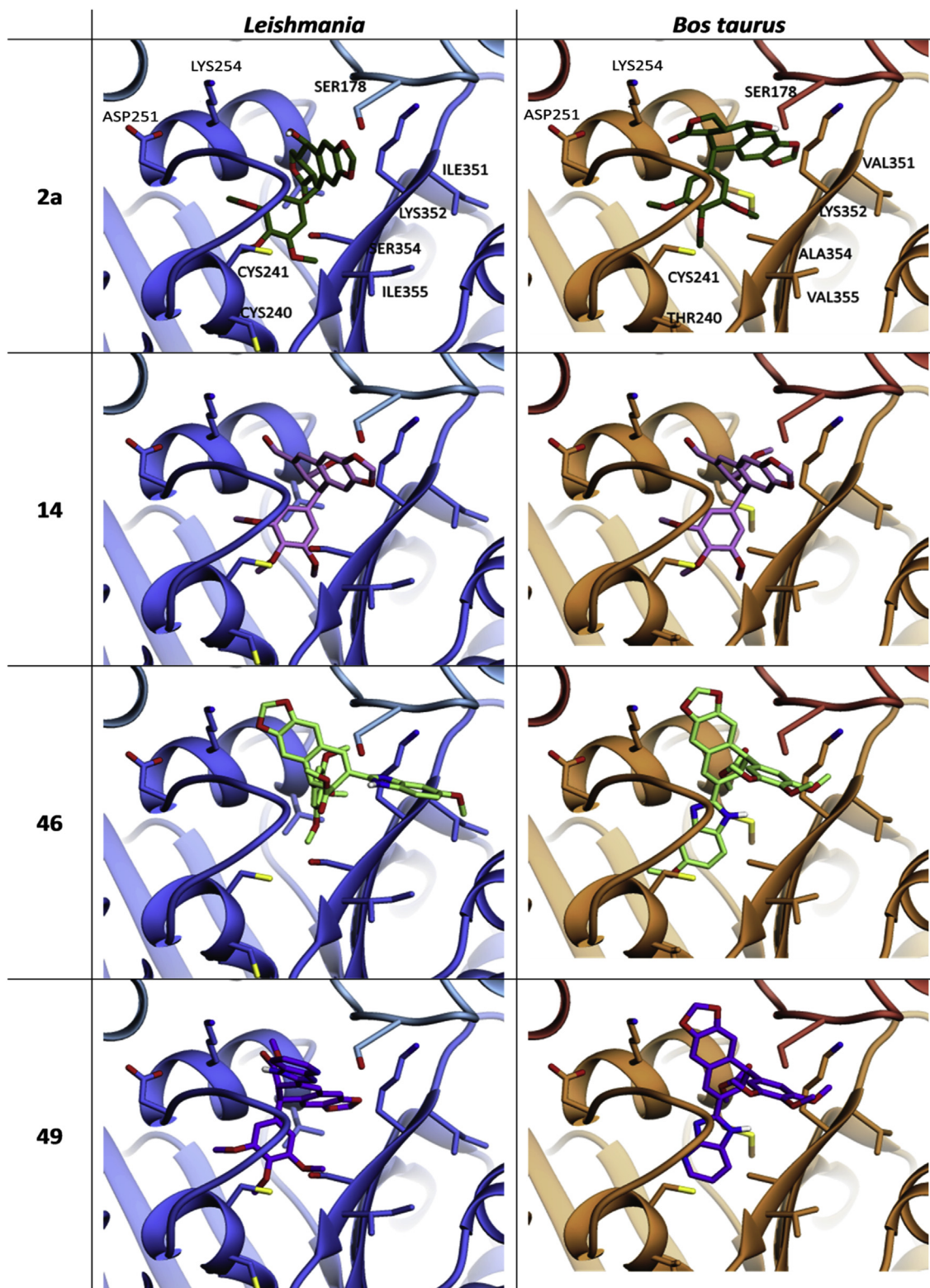


Fig. 3. Calculated docking of podophyllotoxin (2a), podophyllic aldehyde (14) and the lignan-heterocycle hybrids (46) and (49), as representative bioactive compounds of this research, in the colchicine site of *L. infantum* (left panels) and *Bos taurus* tubulins (right panels). The program used for calculating the figure was AutoDock 4.2 software.

5. Conclusions

In summary, we have evaluated and analyzed the anti-leishmanial effects of 53 podophyllotoxin and podophyllic

aldehyde derivatives on both promastigotes and splenocytes naturally infected with amastigotes of *L. infantum*. Several discrepancies found between antileishmanial and antitubulin results displayed by compounds with different but close structures,

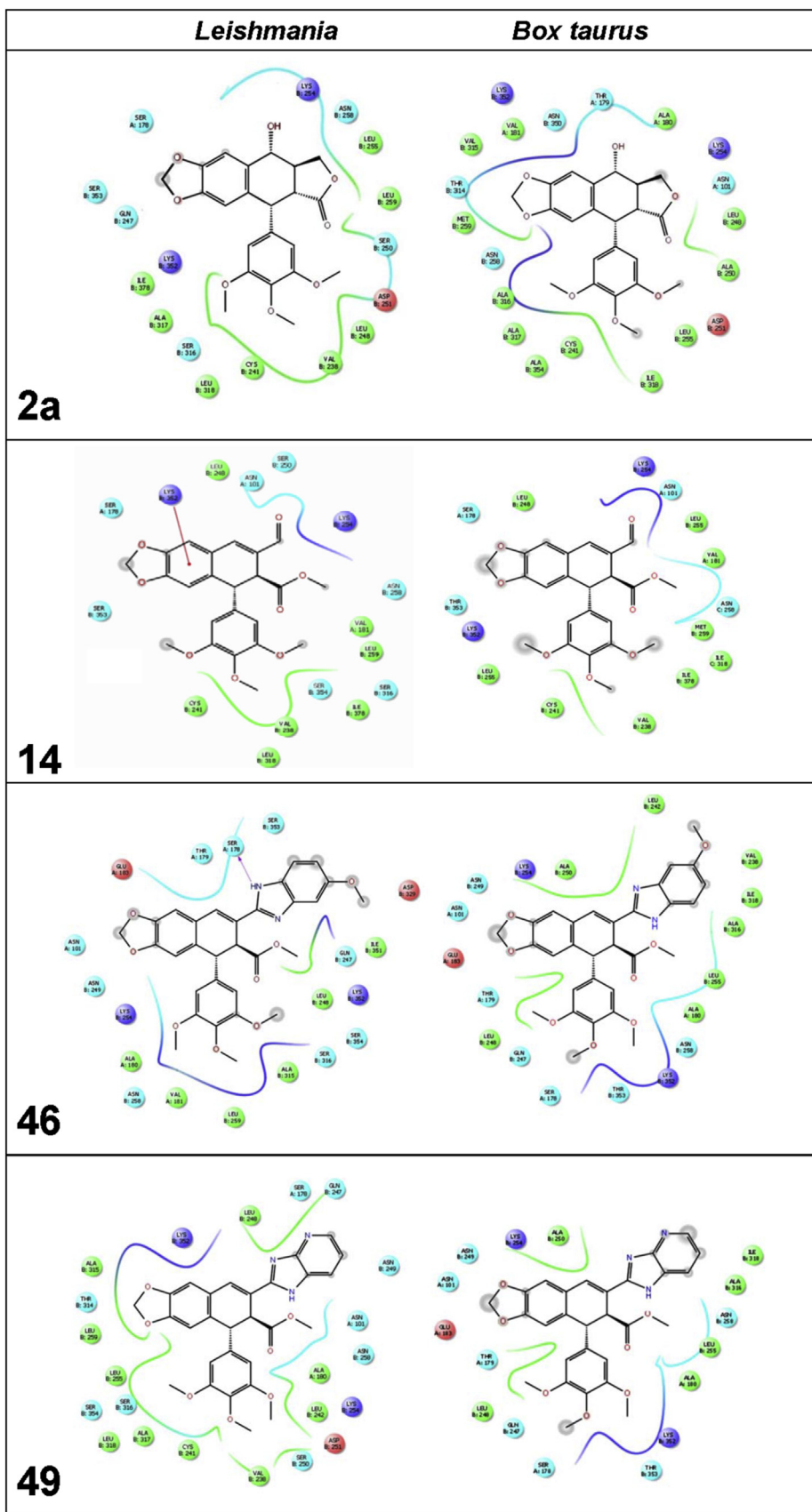


Fig. 4. 2D protein ligand interaction maps for compounds 2a (podophyllotoxin), 14 (podophyllic aldehyde), 46 (lignan-benzimidazole hybrid) and 49 (lignan-imidazopyridine hybrid) on *Leishmania* (left) and *Bos taurus* (right) tubulins. Amino acids at a distance lesser than 4 Å are marked as follows: cationic (purple), anionic (red), hydrophobic (green), polar (blue), and parts exposed to solvent (grey). (For interpretation of the references to colour in this figure legend, the reader is referred to the web version of this article.)

suggest the existence of another mechanism of action, alternative or complementary to the inhibition of tubulin polymerization as responsible for the antileishmanial effects. This evidence merits further studies to confirm it and explain how these compounds are acting on a different therapeutic target, also aiming to progress in the development of new and better drugs against this deadly and still neglected disease.

Conflict of interest

There are none.

Acknowledgements

This collaborative research was carried out under the auspices of the RICET-ISCIH Network (Groups: RD12/0018/0002, RD16/0027/0008 and RD06/0021/1004) and the CYTED Program (214RT0482). It was supported by Ministerio de Economía y Competitividad (MINECO; AGL 2010-16078/GAN; CTQ 2015-68175-R), co-financed by Fondo Social Europeo, Instituto de Salud Carlos III-Feder (PI12/00104) and Junta de Castilla y León (Grants to: Gr208, SA221U13 and Gr238, LE182U13).

Appendix A. Supplementary data

Supplementary data related to this article can be found at <http://dx.doi.org/10.1016/j.ijpddr.2017.06.003>.

References

Abad, A., Lopez-Perez, J.L., del Olmo, E., Garcia-Fernandez, L.F., Francesch, A., Trigili, C., Barasoain, I., Andreu, J.M., Díaz, J.F., San Feliciano, A., 2012. Synthesis and antimitotic and tubulin interaction profiles of novel pinacol derivatives of podophyllotoxins. *J. Med. Chem.* 55, 6724–6737.

Balaña-Fouce, R., Reguera, R.M., Cubría, J.C., Ordóñez, D., 1998. The pharmacology of leishmaniasis. *Gen. Pharmacol.* 30, 435–443.

Balaña-Fouce, R., Prada, C.F., Requena, J.M., Cushman, M., Pommier, Y., Álvarez-Velilla, R., Escudero-Martínez, J.M., Calvo-Álvarez, E., Pérez-Pertejo, Y., Reguera, R.M., 2012. Indotecan (LMP400) and AM13-55: two novel indenoisoquinolines show potential for treating visceral leishmaniasis. *Antimicrob. Agents Chemother.* 56, 5264–5270.

Beaumier, C.M., Gillespie, P.M., Hotez, P.J., Bottazzi, M.E., 2013. New vaccines for neglected parasitic diseases and dengue. *Trans. Res.* 162, 144–155.

Benkert, P., Tosatto, S.C., Schomburg, D., 2008. QMEAN: a comprehensive scoring function for model quality assessment. *Proteins* 71, 261–277.

Benkert, P., Tosatto, S.C., Schwede, T., 2009. QMEANclust: estimation of protein model quality by combining a composite scoring function with structural density information. *BMC Struct. Biol.* 9, 35.

Benkert, P., Biasini, M., Schwede, T., 2011. Toward the estimation of the absolute quality of individual protein structure models. *Bioinformatics* 27, 343–350.

Bhattacharya, S.K., Sinha, P.K., Sundar, S., Thakur, C.P., Jha, T.K., Pandey, K., Das, V.R., Kumar, N., Lal, C., Verma, N., Singh, V.P., Ranjan, A., Verma, R.B., Anders, G., Sindermann, H., Ganguly, N.K., 2007. Phase 4 trial of miltefosine for the treatment of Indian visceral leishmaniasis. *J. Infect. Dis.* 196, 591–598.

Calvo-Álvarez, E., Guerrero, N.A., Álvarez-Velilla, R., Prada, C.F., Requena, J.M., Punzón, C., Llamas, M.A., Arévalo, F.J., Rivas, L., Fresno, M., Pérez-Pertejo, Y., Balaña-Fouce, R., Reguera, R.M., 2012. Appraisal of a *Leishmania major* strain stably expressing mCherry fluorescent protein for both in vitro and in vivo studies of potential drugs and vaccine against cutaneous leishmaniasis. *PLoS Negl. Trop. Dis.* 6, e1927.

Castro, M.A., Miguel del Corral, J.M., Gordaliza, M., Grande, C., Gómez-Zurita, A., García-Grávalos, D., San Feliciano, A., 2003. Synthesis and cytotoxicity of podophyllotoxin analogues modified in the A ring. *Eur. J. Med. Chem.* 38, 65–74.

Castro, M.A., Miguel del Corral, J.M., Gordaliza, M., García, P.A., Gómez-Zurita, M.A., García-Grávalos, M.D., de la Iglesia-Vicente, J., Gajate, C., An, F., Mollinedo, F., San Feliciano, A., 2004. Synthesis and biological evaluation of new selective cytotoxic cyclolignans derived from podophyllotoxin. *J. Med. Chem.* 47, 1214–1222.

Castro, M.A., Miguel del Corral, J.M., García, P.A., Rojo, M.V., de la Iglesia-Vicente, J., Mollinedo, F., Cuevas, C., San Feliciano, A., 2010. Synthesis and biological evaluation of new podophyllaldehyde derivatives with cytotoxic and apoptosis-inducing activities. *J. Med. Chem.* 5, 983–993.

Castro, M.A., Miguel del Corral, J.M., García, P.A., Rojo, M.V., Bento, A.C., Mollinedo, F., Francesch, A.M., San Feliciano, A., 2012. Lignopurines: a new family of hybrids between cyclolignans and purines. Synthesis and biological

evaluation. *Eur. J. Med. Chem.* 58, 377–389.

Chan, M.M., Fong, D., 1990. Inhibition of leishmanias but not host macrophages by the antitubulin herbicide trifluralin. *Science* 249, 924–926.

Chan, M.M., Triemer, R.E., Fong, D., 1991. Effect of the anti-microtubule drug oryzalin on growth and differentiation of the parasitic protozoan *Leishmania mexicana*. *Differentiation* 46, 15–21.

Chan, M.M., Grogl, M., Chen, C.C., Bienen, E.J., Fong, D., 1993a. Herbicides to curb human parasitic infections: *in vitro* and *in vivo* effects of trifluralin on the trypanosomatid protozoans. *Proc. Natl. Acad. Sci. U. S. A.* 90, 5657–5661.

Chan, M.M., Tzeng, J., Emge, T.J., Ho, C.T., Fong, D., 1993b. Structure-function analysis of antimicrotubule dinitroanilines against promastigotes of the parasitic protozoan *Leishmania mexicana*. *Antimicrob. Agents. Chemother.* 37, 1909–1913.

Croft, S.L., Olliaro, P., 2011. Leishmaniasis chemotherapy—challenges and opportunities. *Clin. Microbiol. Infect.* 17, 1478–1483.

Dumontet, C., Sikic, B.I., 1999. Mechanisms of action of and resistance to antitubulin agents: microtubule dynamics, drug transport, and cell death. *J. Clin. Oncol.* 17, 1061–1070.

Fiser, A., Do, R.K., Sali, A., 2000. Modelling of loops in protein structures. *Protein Sci.* 9, 1753–1773.

Gordaliza, M., Castro, M.A., Miguel del Corral, J.M., López-Vázquez, M.L., García, P.A., García-Grávalos, M.D., San Feliciano, A., 2000. Synthesis and antineoplastic activity of cyclolignan aldehydes. *Eur. J. Med. Chem.* 35, 691–698.

Hawkins, T., Mirigian, M., Selcuk Yasar, M., Ross, J.L., 2010. Mechanics of microtubules. *J. Biomech.* 43, 23–30.

Humphrey, W., Dalke, A., Schulten, K., 1996. VMD: visual molecular dynamics. *J. Mol. Graph.* 14, 33–38, 27–28.

Kaur, R., Kaur, G., Gill, R.K., Soni, R., Bariwal, J., 2014. Recent developments in tubulin polymerization inhibitors: an overview. *Eur. J. Med. Chem.* 87, 89–124.

Kohl, L., Gull, K., 1998. Molecular architecture of the trypanosome cytoskeleton. *Mol. Biochem. Parasitol.* 93, 1–9.

Laskowski, R.A., MacArthur, M.W., Moss, D.S., Thornton, J.M., 1993. PROCHECK: a program to check the stereochemical quality of protein structures. *J. Appl. Cryst.* 26, 283–291.

López-Pérez, J.L., del Olmo, E., de Pascual-Teresa, B., Abad, A., San Feliciano, A., 2004. Synthesis and cytotoxicity of hydrophobic esters of podophyllotoxins. *Bioorg. Med. Chem. Lett.* 14, 1283–1286.

Luis, L., Serrano, M.L., Hidalgo, M., Mendoza-Leon, A., 2013. Comparative analyses of the beta-tubulin gene and molecular modelling reveal molecular insight into the colchicine resistance in kinetoplastids organisms. *Biomed. Res. Int.* 2013, 843748.

Mandal, G., Mandal, S., Sharma, M., Charret, K.S., Papadopoulou, B., Bhattacharjee, H., Mukhopadhyay, R., 2015. Species-specific antimonial sensitivity in Leishmania is driven by post-transcriptional regulation of AQP1. *PLoS Negl. Trop. Dis.* 9, e0003500.

Marti-Renom, M.A., Stuart, A.C., Fiser, A., Sanchez, R., Melo, F., Sali, A., 2000. Comparative protein structure modeling of genes and genomes. *Annu. Rev. Biophys. Biomol. Struct.* 29, 291–325.

Massarotti, A., Coluccia, A., Silvestri, R., Sorba, G., Brancale, A., 2012. The tubulin colchicine domain: a molecular modelling perspective. *ChemMedChem* 7, 33–42.

Monge-Maillo, B., Lopez-Velez, R., 2013. Therapeutic options for old world cutaneous leishmaniasis and New World cutaneous and mucocutaneous leishmaniasis. *Drugs* 73, 1889–1920.

Morris, G.M., Huey, R., Lindstrom, W., Sanner, M.F., Belew, R.K., Goodsell, D.S., Olson, A.J., 2009. AutoDock4 and AutoDockTools4: automated docking with selective receptor flexibility. *J. Comput. Chem.* 30, 2785–2791.

Petersen, E.F., Goddard, T.D., Huang, C.C., Couch, G.S., Greenblatt, D.M., Meng, E.C., Ferrin, T.E., 2004. UCSF Chimera a visualization system for exploratory research and analysis. *J. Comp. Chem.* 25, 1605–1612.

Prota, A.E., Danel, F., Bachmann, F., Bargsten, K., Buey, R.M., Pohlmann, J., Reinelt, S., Lane, H., Steinmetz, M.O., 2014. The novel microtubule-destabilizing drug BAL27862 binds to the colchicine site of tubulin with distinct effects on microtubule organization. *J. Mol. Biol.* 426, 1848–1860.

Ravelli, R.B., Gigant, B., Curmi, P.A., Jourdain, I., Lachkar, S., Sobel, A., Knossow, M., 2004. Insight into tubulin regulation from a complex with colchicine and a stathmin-like domain. *Nature* 428, 198–202.

Reguera, R.M., Calvo-Álvarez, E., Álvarez-Velilla, R., Balaña-Fouce, R., 2014. Target-based vs. phenotypic screenings in Leishmania drug discovery: a marriage of convenience or a dialogue of the deaf? *Int. J. Parasitol. Drugs Drug Resist* 4, 355–357.

Sacks, D.L., Perkins, P.V., 1984. Identification of an infective stage of Leishmania promastigotes. *Science* 223, 1417–1419.

Sali, A., Blundell, T.L., 1993. Comparative protein modelling by satisfaction of spatial restraints. *J. Mol. Biol.* 234, 779–815.

Schwede, T., Kopp, J., Guex, N., Peitsch, M.C., 2003. Swiss-model: an automated protein homology-modeling server. *Nucleic Acids Res.* 31, 3381–3385. <http://swissmodel.expasy.org/SWISS-MODEL.html>.

Seeback, T., Hemphill, A., Lawson, D., 1990. The cytoskeleton of trypanosomes. *Parasitol. Today* 6, 49–52.

Seifert, K., Matu, S., Pérez-Victoria, F.J., Castanys, S., Gamarro, F., Croft, S.L., 2003. Characterisation of *Leishmania donovani* promastigotes resistant to hexadecylphosphocholine (miltefosine). *Int. J. Antimicrob. Agents* 22, 380–387.

Sundar, S., Chakravarty, J., 2010. Antimony toxicity. *Int. J. Environ. Res. Public Health* 7, 4267–4277.

ter Haar, E., Rosenkranz, H.S., Hamel, E., Day, B.W., 1996. Computational and

- molecular modelling evaluation of the structural basis for tubulin polymerization inhibition by colchicine site agents. *Bioorg. Med. Chem.* 4, 1659–1671.
- Traub-Cseko, Y.M., Ramalho-Ortigao, J.M., Dantas, A.P., de Castro, S.L., Barbosa, H.S., Downing, K.H., 2001. Dinitroaniline herbicides against protozoan parasites: the case of *Trypanosoma cruzi*. *Trends Parasitol.* 17, 136–141.
- Vindya, N.G., Sharma, N., Yadav, M., Ethiraj, K.R., 2015. Tubulins - the target for anticancer therapy. *Curr. Top. Med. Chem.* 15, 73–82.
- Werbovetz, K.A., 2002. Promising therapeutic targets for antileishmanial drugs. *Expert. Opin. Ther. Targets* 6, 407–422.
- Yakovich, A.J., Ragone, F.L., Alfonzo, J.D., Sackett, D.L., Werbovetz, K.A., 2006. *Leishmania tarentolae*: purification and characterization of tubulin and its suitability for antileishmanial drug screening. *Exp. Parasitol.* 114, 289–296.
- Yang, Z., Lasker, K., Schneidman-Duhovny, D., Webb, B., Huang, C.C., Pettersen, E.F., Goddard, T.D., Meng, E.C., Sali, A., Ferrin, T.E., 2012. UCSF Chimera, MODELLER, and IMP: an integrated modelling system. *J. Struct. Biol.* 179, 269–278.